Surface and Bulk Contribution to Cu(111) Quantum Efficiency

E. Pedersoli,[1,*] C. M. R. Greaves,[1] W. Wan,[1] C. Coleman-Smith,[1] H. A. Padmore,[1] S. Pagliara,[2] A. Cartella,[2] F. Lamarca,[2] G. Ferrini,[2] G. Galimberti,[2] M. Montagnese,[2] S. dal Conte,[2] and F. Parmigiani[3,4]

[1]*Lawrence Berkeley National Laboratory, One Cyclotron Road, Berkeley, CA 94720 USA*
[2]*Dipartimento di Matematica e Fisica, Università Cattolica, Via Musei 41, I-25121 Brescia*
[3]*Dipartimento di Fisica, Università degli studi di Trieste, Piazzale Europa 1, I-34127 Trieste*
[4]*Sincrotrone Trieste S.p.A. Strada Statale 14, km 163.5, I-34012 Basovizza (TS)*

(Dated: October 29, 2008)

The quantum efficiency QE of Cu(111) is measured for different impinging light angles with photon energies just above the work function. We observe that the vectorial photoelectric effect, an enhancement of the quantum efficiency due to illumination with light with an electric vector perpendicular to the sample surface, is stronger in the more surface sensitive regime. This can be explained by a contribution to photoemission due to the variation of the electromagnetic potential at the surface. The contributions of bulk and surface electrons can then be determined.

Photoemission from metals has been studied for more than a century both from the experimental and the theoretical point of view [1, 2]. Many aspects of this phenomenon are well understood and explained, but others, such as quantitative theoretical prediction of relative peak intensities [3] and total photoemission yield [4], need further development. Not only is this of theoretical interest, it has practical application in the design of photocathodes for Free Electron Lasers (FELs) and ultrafast electron diffraction.

In this letter we show experimental measurements of the total photoemission quantum efficiency's QE dependence on the incidence angle θ of the impinging light. Cu(111) was chosen as a sample due to its robust nature and its well known and experimentally verified band structure [5–7]: this allows us, through tuning the incident photon energy $h\nu$, to control the relative proportions of surface and bulk electrons emitted. As expected [8, 9], the three step model [10], which predicts a QE proportional to the absorbed part $(1 - R(\theta))$ of the incident photon energy, needs to be corrected to account for the more effective emission from the electric-field component perpendicular to the sample's surface. Since the intensity of this behavior, known as the vectorial photoelectric effect, increases with the surface sensitivity of the emission process, it is directly related to the well-known surface photoelectric effect [11–13], due to the variation at the sample surface of the perpendicular component $A_\perp$ of the light electromagnetic potential.

The quantum efficiency was measured as a function of the incidence angle θ of the impinging photons in the range $-63° < \theta < 57°$ with 5° steps ($\theta = 0°$ indicates normal incidence) for two different values of the photon energy $h\nu_1 = 5.44$ eV and $h\nu_2 = 5.74$ eV; data are compared to results of Ref. 9, obtained with $h\nu_3 = 6.28$ eV.

Considering the Cu(111) projected band structure shown in Fig. 1, with work function $\phi = 4.94$ eV, surface state and bulk band gap bottom binding energies $E_{SS} = 5.35$ eV and $E_{BG} = 5.8$ eV respectively at $k_\parallel = 0$, an estimation of the probed initial states can be made for each photon energy. If we assume vacuum free electrons as the final states of the photoemission process, all the Shockley surface state and only a small number of bulk electrons can be excited by the $h\nu_1 = 5.44$ eV photons

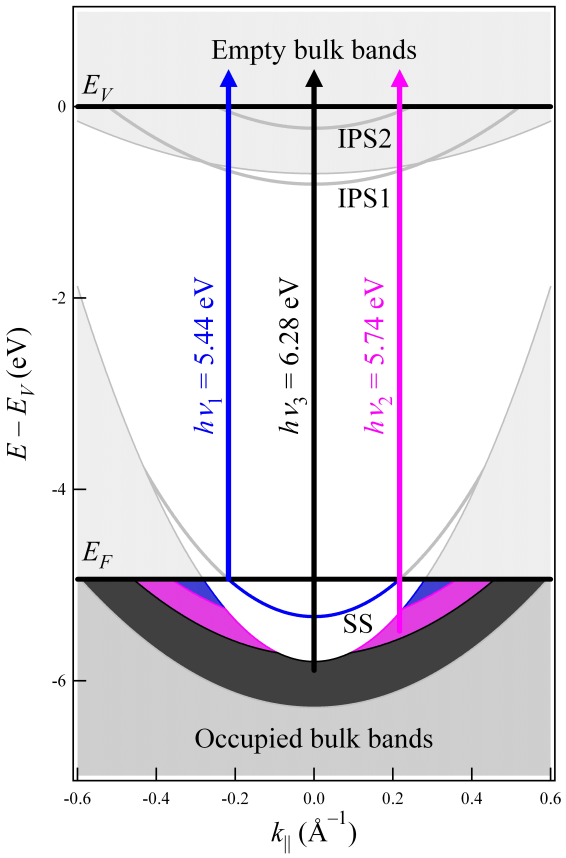

FIG. 1: Cu(111) band structure [5–7]. States probed by photons of energy $h\nu_1 = 5.44$ eV, $h\nu_2 = 5.74$ eV and $h\nu_3 = 6.28$ eV are highlighted in blue, states probed by $h\nu_2$ and $h\nu_3$ are highlighted in violet, states probed by $h\nu_3$ only are highlighted in black. $h\nu_1$, exciting all the surface state (SS) and only a few bulk states, is the most surface sensitive; $h\nu_3$ is more bulk sensitive, probing more bulk bands.

and are highlighted in blue in Fig. 1. The $h\nu_2 = 5.74$ eV photons also probe the violet colored area of the bulk bands, while light with energy $h\nu_3 = 6.28$ eV is even more bulk sensitive, exciting electrons from the black highlighted states as well as the others. Crystal empty bands just above the vacuum level have to be considered as intermediate states in the photoemission process, but the effects of this step are neglected, since these bands present no gaps and a uniform density of states in this region.

The number of excited electrons in a photoemission process involving an initial state $|i\rangle$ and a final state $|f\rangle$, whose momentum matrix element is $\langle i|\mathbf{p}|f\rangle = \mathbf{p}_{if}$, excited by an electromagnetic vector potential $\mathbf{A}$, is expected to be proportional to $|\mathbf{A}\cdot\mathbf{p}_{if}|^2$. The predicted total yield, obtained by integrating this quantity over all the possible $|i\rangle$ and $|f\rangle$, is supposed to be isotropic for regular systems like noble metals bulk bands, and proportional to $|\mathbf{A}|^2$ inside the sample. As such, in the three step model [10], the only dependence of the yield on the incidence light is expected to be the total absorbed energy. This is proportional to the incident light intensity and to $(1-R(\theta))$, where $R(\theta)$ is the reflectivity calculated from the Fresnel laws [14].

This prediction is not confirmed by Cu(111) data obtained for p polarized light: a further assumption is necessary. The absorbed energy $\varepsilon_{p\perp}$ due to the electromagnetic potential component $A_\perp$ perpendicular to the surface appears to be more efficient than ε_s and $\varepsilon_{p\parallel}$ due to the parallel component $A_\parallel$. This results in a quantum efficiency dependence on the incidence angle that can be expressed for s and p polarized light respectively by

$$\frac{QE_s(\theta)}{QE(0)} = \frac{\varepsilon_s(\theta)}{\varepsilon_s(0)} \qquad (1)$$

and

$$\frac{QE_p(\theta)}{QE(0)} = \frac{\varepsilon_{p\parallel}(\theta)}{\varepsilon_{p\parallel}(0)} + r\frac{\varepsilon_{p\perp}(\theta)}{\varepsilon_{p\parallel}(0)}. \qquad (2)$$

$QE(0)$ and r are fit parameters; r is used to measure the ratio between the effectivenesses of perpendicular and parallel light fields [8, 9].

An amplified Ti:Sapphire laser was used as the light source in this experiment, providing 150 fs 790 nm pulses with an average light power of 500 mW at 1 kHz repetition rate. The output was split into two beams: the first pumping a parametric amplifier that provided tunability in the near infrared, the second undergoing a process of third harmonic generation obtained with two stages of sum frequency generation in type I BBO crystals. After a delay line that provides temporal coincidence, the beams converge on a third crystal for sum frequency generation providing the desired wavelengths. The sample total current on a picoammeter and the light intensity of a beam reflection on a calibrated photodiode were measured to provide the experimental data.

The experiment was performed in an ultrahigh vacuum chamber with base pressure 2×10^{-10} mbar at room temperature on a Cu(111) crystal polished with cycles of Ar^+ sputtering at 1 keV kinetic energy and annealing at 750 K. The sample cleanliness was tested online by acquiring photoemission spectra through a time of flight analyzer and checking the sharpness of the L gap surface state and the work function value.

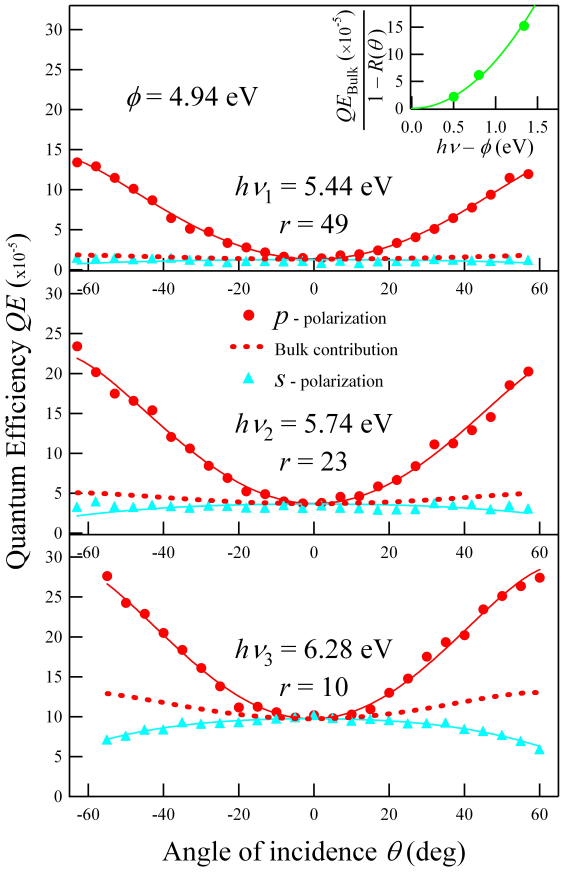

FIG. 2: Quantum efficiency data as a function of the incident light angle θ for the three different photon energies are fitted using Eq. 1, 2; the bottom panel shows data from Ref. 9. The red dotted lines represent the prediction for the bulk contribution, proportional to the absorbed part $(1-R(\theta))$ of light energy. The top right panel shows the bulk quantum efficiency fitted by the Fowler law Eq. 3.

Quantum efficiency data are shown in Fig. 2, compared to results of Ref. 9 and fitted by Eq. 1, 2 [15]; the obtained values of the parameter r ($r = 49$ for $h\nu_1 = 5.44$ eV, $r = 23$ for $h\nu_2 = 5.74$ eV, $r = 10$ for $h\nu_3 = 6.28$ eV) show that the vectorial effect is stronger when the photoemission process is more surface sensitive. Since the same effect is observed on polycrystalline samples on which surface states are not observed by photoemission spectroscopy [9], it can not be explained just by the dipole selection rules for photoemission from the surface state, which forbid electrons to be excited by electric fields par-

allel to the sample surface. An explanation is found in the surface photoemission effect [11–13]: since entering a solid of permittivity ε the perpendicular component of the electromagnetic potential $\mathbf{A}$ varies from $A_\perp/\varepsilon$ to $A_\perp$ in a distance d across the surface, an additional term proportional to $|\nabla\cdot\mathbf{A}|^2 \cong [(\varepsilon-1)/\varepsilon d]^2|A_\perp|^2$ contributes to the photoemission process.

We can divide the quantum efficiency for p polarized light into a bulk contribution proportional to the absorbed light energy $(1-R(\theta))$, shown as a dotted red line in Fig. 2, and a surface contribution calculated subtracting the bulk contribution from the total quantum efficiency and shown in Fig. 3. In this picture (for the bulk we hold the fit parameter to $r=1$) the residual value $(r-1)$ represents the relative efficiency of surface $|\nabla\cdot\mathbf{A}|^2$ and bulk $|\mathbf{A}\cdot\mathbf{p}_{if}|^2$ contributions.

The amount of probed bulk bands strongly depends on the wavelength: since a higher photon energy can excite more varied states, as shown in Fig. 1, the bulk quantum efficiency is expected to vary as the square of the absorbed excess energy, following the Fowler law [16]

$$\frac{QE_{Bulk}(\theta)}{1-R(\theta)} = \frac{QE_{Bulk}(0)}{1-R(0)} \propto (h\nu-\phi)^2, \qquad (3)$$

where the ratio in the left term is independent of the incidence angle θ. The fit presented in the top right panel of Fig. 2 shows a good agreement with the law and is not strongly affected by the band-gap induced asymmetry.

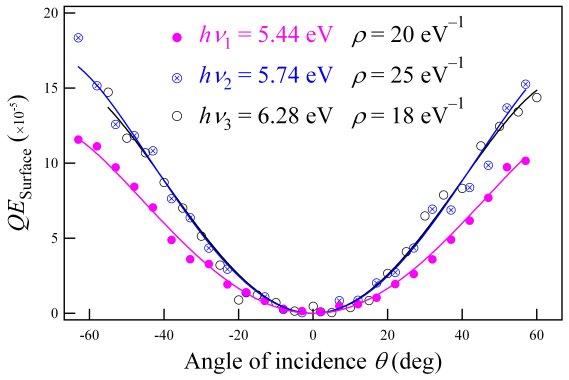

FIG. 3: Surface quantum efficiency data as a function of the incidence light angle θ for the three different photon energies are fitted using Eq. 5.

The contribution to quantum efficiency due to electrons excited from the surface state, on the contrary, does not follow Fowler's law. Since each of the three considered photon energies can excite electrons from the whole Shockley state, higher energy photons don't have any other surface state to probe. The surface electron yield is therefore expected to be proportional to $\varepsilon_{p\perp}(\theta)$, the absorbed energy due to $A_\perp$; we define the fit parameter ρ as the proportionality constant, whose dimensions are eV^{-1}. Dividing by the number of impinging photons n_i, we can write the surface quantum efficiency for p polarized light as

$$QE_{Surface}(\theta) = \rho\frac{\varepsilon_{p\perp}(\theta)}{n_i} = \rho\frac{n_t h\nu}{n_i}\frac{\varepsilon_{p\perp}(\theta)}{\varepsilon_{p\perp}(\theta)+\varepsilon_{p\parallel}(\theta)}, \quad (4)$$

where n_t is the number of transmitted photons, $n_t h\nu$ and $(\varepsilon_{p\perp}(\theta)+\varepsilon_{p\parallel}(\theta))$ are both the total absorbed energy. Considering that $n_t/n_i = 1-R(\theta)$, we can fit surface quantum efficiency data with the formula

$$QE_{Surface}(\theta) = \rho(1-R(\theta))h\nu\frac{\varepsilon_{p\perp}(\theta)}{\varepsilon_{p\perp}(\theta)+\varepsilon_{p\parallel}(\theta)}, \quad (5)$$

obtaining for the fit parameters values $\rho = 20$ eV^{-1} for $h\nu_1 = 5.44$ eV, $\rho = 25$ eV^{-1} for $h\nu_2 = 5.74$ eV, $\rho = 18$ eV^{-1} for $h\nu_3 = 6.28$ eV. The three values are consistent within a relative error of $\pm 20\%$.

The Quantum efficiency of Cu(111) was analyzed at different impinging light angles for several photon energies with different surface sensitiveness. The observed vectorial photoelectric effect is stronger when in the more surface dominated regime: we explain this by breaking down the photoemission into bulk and surface components. The anisotropy of the surface contribution, proportional to $\nabla\cdot\mathbf{A}$, is then due to the variation of the perpendicular component of the electromagnetic potential at the surface.

This work was supported by the U.S. Department of Energy under Contract No. DE-AC02-05CH11231.

* e-mail:EPedersoli@lbl.gov

[1] S. D. Kevan, *Angle-Resolved Photoemission* (Elsevier, Amsterdam, 1992).
[2] S. Hüfner, *Photoelectron Spectroscopy Principles and Applications, 3rd edition* (Springer, Berlin, 1995).
[3] N. V. Smith, R. L. Bembow, and Z. Hurych, Phys. Rev. B **21**, 4331 (1980).
[4] P. Gartland and B. Slagsvold, Phys. Rev. B **12**, 4047 (1975).
[5] A. Goldmann, V. Dose, and G. Borstel, Phys. Rev. B **32**, 1971 (1985).
[6] S. Caravati *et al.*, Surf. Sci. **600**, 3901 (2006).
[7] R. C. Weast and M. J. Astle, *Hand Book of Chemistry and Physics* (CRC Press, Boca Raton, Florida, 1982).
[8] R. M. Broudy, Phys. Rev. B **3**, 3641 (1971).
[9] E. Pedersoli *et al.*, Appl. Phys. Lett. **87**, 081112 (2005).
[10] C. N. Berglund and W. E. Spicer, Phys. Rev. **136**, A1030 (1964).
[11] P. J. Feibelman, Phys. Rev. B **12**, 1319 (1975).
[12] J. G. Endriz, Phys. Rev. B **7**, 3464 (1972).
[13] R. Raşeev and D. Bejan, Surf. Sci. **528**, 196 (2003).
[14] H. Y. Fan, Phys. Rev. **68**, 43 (1945).
[15] Indexes of refraction $n = 1.30 + 1.77i$ for $h\nu_1 = 5.44$ eV, $n = 1.13 + 1.69i$ for $h\nu_3 = 5.74$ eV and $n = 0.98 + 1.49i$ for $h\nu_3 = 6.28$ eV are used [17].
[16] R. H. Fowler, Phys. Rev. **38**, 45 (1931).
[17] *Handbook of optical constants of solids* (Academic Press, Orlando, Florida, 1985).